•特约稿•

DOI:10.15961/j.jsuese.201800398

用于火电厂减震的变质量MTMD基于可靠度的优化

戴靠山[1,2],李伯维[2],李卉颖[2],王健泽[2],李　昂[2],刘　恺[2],*TESFAMARIAM Solomon*[3]

(1.四川大学 土木工程系,四川 成都 610065;2.同济大学 土木工程防灾国家重点实验室,上海 200092;
3.School of Eng., Univ. of British Columbia, British Columbia, Canada V1V1V7)

摘　要:提出了一种针对变质量的非传统多调谐阻尼器(MTMD)基于可靠度的优化设计方法。其中主结构部分考虑多阶模态,MTMD则考虑为集中质量。地震动激励采用金井清模型,利用状态空间法提高计算效率。地震危险性则依据地震动衰减关系和Gutenberg-Richter模型模拟。定义危险性、主结构与多调谐阻尼器相关参数均为随机变量,通过考虑结构多维输出及对应限值,并结合激励与结构随机性得到结构绝对失效概率,并进一步以绝对失效概率为目标函数形成优化问题,通过求解变质量MTMD最优解进行设计。本文将该方法应用于带多煤斗的火电厂房煤斗隔震设计。其中,煤斗隔震形成MTMD,而煤斗内部储煤量变化则形成变质量MTMD。采用拉丁超立方抽样法生成样本,研究确定了合适样本数。通过选取结构角柱位移角作为结构响应,采用规范限值计算失效概率。利用基因算法求解了该优化问题并得到了最优设计与对应的失效概率。本文进一步对比了平动隔震体系和摆隔震体系。研究表明,尽管摆体系的频率与质量不相关,其失效概率并未优于平动隔震体系;且摆体系摆动圆弧曲率的变异系数对结构失效概率影响不大,规律不明显。最后,将煤斗与主结构碰撞亦考虑为失效事件,考虑了煤斗碰撞问题。本文所提出的设计方法基于可靠度,直接以降低结构失效概率为目标,可同时考虑结构多维输出以及煤斗与主结构相对位移,并对应地考虑多个响应限值,将多个响应综合为一个失效概率,避免了计算量巨大的多目标优化。

关键词:非传统调谐阻尼器;质量不确定;火电厂减震;可靠度;优化设计

中图分类号:TU271.1;TU391;TU311.3　　**文献标志码**:A　　**文章编号**:2096-3246(2018)03-0082-09

Reliability Based Mass Uncertain Nonconventional Multiple Tuned Mass Damper Optimization for Thermal Power Plant

DAI Kaoshan[1,2], *LI Bowei*[2], *LI Huiying*[2], *WANG Jianze*[2], *LI Ang*[2], *LIU Kai*[2], *TESFAMARIAM Solomon*[3]

(1.Dept. of Civil Eng., Sichuan Univ., Chengdu 610065, China; 2.State Key Lab. of Disaster Reduction in Civil Eng., Tongji Univ., Shanghai 200092, China;
3.School of Eng., Univ. of British Columbia, British Columbia, Canada V1V1V7)

Abstract: A reliability-based optimization design framework for mass uncertain nonconventional multiple tuned mass damper (MTMD) systems was proposed. The structure was modelled as a hybrid-model with multiple tuned mass dampers simplified as lumped masses. Seismic excitation was modelled by the Kanai-Tajimi filtered white noise. State-space representation was adopted to enhance the simulation efficiency. Attenuation relationship and truncated Gutenberg-Richter relationship were used for hazard condition definition. Multiple parameters associated with hazards, the main structure, and multiple tuned mass dampers were considered to be random. The objective function was defined following the unconditional failure probability with multiple limit state bounds, incorporating both structural and excitation uncertainties. A case study based on a thermal power plant with multiple scuttles was carried out to illustrate the framework. The Latin Hypercube Sampling (LHS) method was implemented to reduce the sample size. Drifts of corner columns were considered as structural responses and code limits were set to assess structural failures. By using genetic algorithm, an optimum design was obtained. A parametric study was further performed to study the influence of isolation system type and seismic gap, along with which the pendulum system and collision problem were investigated. It is found that scuttle isolation

收稿日期:2018 – 03 – 07

基金项目:上海市国际合作资助项目(16510711300);四川省国际合作资助项目(18GJHZ0111);国家自然科学基金资助项目(U1710111);中央高校基本科研业务费专项资金资助项目;中国电力建设集团科研资助项目(KJ-2016-095)

作者简介:戴靠山(1977—),男,教授,博士. 研究方向:能源基础设施韧性防灾. E-mail:kdai@scu.edu.cn

网络出版时间:2018 – 05 – 05 17 : 44 : 00　　**网络出版地址**:http://kns.cnki.net/kcms/detail/51.1773.TB.20180505.1744.005.html

via the pendulum system is not a better design as expected since the failure probability is not sensitive to the variance of pendulum curvature. By considering scuttle collision as additional factor, the failure probability with the inclusion of this constraint was obtained. The proposed design method is based on structural reliability, which is capable of considering multi-dimensional outputs and corresponding response limits and integrating multiple structural responses into one failure probability.

Key words: nonconventional tuned mass damper;mass uncertainty;thermal power plant seismic mitigation;reliability;optimization deisgn

Thermal power plant is an important life line structure[1]. Maintaining its workability during and after earthquakes can be essential for people's life and recovery[1]. However, due to the functional requirements, thermal power plants are usually designed as complex structures with various irregularities[2–6]. Besides, typically thermal power plants consists heavy coal scuttles at relatively high floors, which may generate significant inertial force and be detrimental to the structural seismic performance[4]. An effective strategy to solve this problem is to convert the scuttles to sub-oscillators and tuning to the main structure, i.e.nonconventional multiple tuned mass damper (NC-MTMD)[5–7].

During the real operational process, the coal storage in the scuttles may change[6–7], which leads to random mass of the tuned mass dampers of NC-MTMD system. This can be classified as a mass uncertain NC-MTMD (MU-NC-MTMD) system. Jensen et al[8]. first investigated TMD system with uncertain mass and proofed the necessities to consider uncertainty during design for moderate (coefficient of variation, CoV=0.15) and high (CoV=0.30) cases.Mass uncertainty was considered in several subsequent studies[9–10]. The mass uncertain tuned mass damper, as a case of isolated roof garden, was investigated in a previous study[10]. The MU-NC-MTMD has multiple sub-oscillators, which is tuned from the original structure instead of tuning additional one, with mass varying from small mass ratio to large mass ratio[6]. Despite NC-MTMD system contains multiple large mass ratio sub-oscillators and therefore has enhanced effectiveness and robustness[6], those may not be a sure thing for MU-NC-MTMD systems. Therefore, performance and optimization of MU-NC-MTMD systems require further study. Besides, several random factors, such as stiffness and damping of sub-oscillators or parameters of main structures, may also lead to a different optimum design[11] and therefore should be considered.

In this paper, a reliability-based optimization design framework for MU-NC-MTMD systems was proposed. Several parameters of hazard, main structures and scuttles were considered to be random. Unconditional failure probability considering multiple limit state bounds was adopted as objective function. A thermal power plant with multiple scuttles was used as a case to illustrate the application of the framework. Latin hypercube sampling (LHS) method was implemented to reduce the sample size needed and sampling size study was performed to determine the appropriate sampling size. Optimum design was obtained and discussed. A parametric study was further performed to study the influence of isolation mechanism and seismic gap. Pendulum MU-NC-MTMD and failure probability considering collision were investigated.

1 Structural model

For a NC-MTMD with a n_M DOF main structure (mass matrix $\boldsymbol{M}$, damping matrix $\boldsymbol{C}$, stiffness matrix $\boldsymbol{K}$) and n_m TMDs (mass matrix $\boldsymbol{m}=\mathrm{diag}(m_j|j=1,2,,n_{\mathrm{m}})$, damping matrix $\boldsymbol{c}=\mathrm{diag}(c_j|j=1,2,,n_{\mathrm{m}})$, stiffness matrix $\boldsymbol{k}=\mathrm{diag}(k_j|j=1,2,,n_{\mathrm{m}})$), the dynamic equation can be expressed as Eq. (1).

$$\begin{bmatrix} \boldsymbol{M}_{n_M\times n_M} & \boldsymbol{O} \\ \boldsymbol{O} & \boldsymbol{m}_{n_m\times n_m} \end{bmatrix}\begin{bmatrix} \ddot{\boldsymbol{X}} \\ \ddot{\boldsymbol{x}} \end{bmatrix}+\begin{bmatrix} \boldsymbol{C}_{n_M\times n_M}+\boldsymbol{l}^{\mathrm{T}}\boldsymbol{c}_{n_m\times n_m}\boldsymbol{l} & \boldsymbol{l}^{\mathrm{T}}\boldsymbol{c}_{n_m\times n_m} \\ \boldsymbol{c}_{n_m\times n_m}\boldsymbol{l} & \boldsymbol{c}_{n_m\times n_m} \end{bmatrix}\begin{bmatrix} \dot{\boldsymbol{X}} \\ \dot{\boldsymbol{x}} \end{bmatrix}+ \\ \begin{bmatrix} \boldsymbol{K}_{n_M\times n_M}+\boldsymbol{l}^{\mathrm{T}}\boldsymbol{k}_{n_M\times n_M}\boldsymbol{l} & \boldsymbol{l}^{\mathrm{T}}\boldsymbol{k}_{n_m\times n_m} \\ \boldsymbol{k}_{n_m\times n_m}\boldsymbol{l} & \boldsymbol{k}_{n_m\times n_m} \end{bmatrix}\begin{bmatrix} \boldsymbol{X} \\ \boldsymbol{x} \end{bmatrix}=\begin{bmatrix} \boldsymbol{M}_{n_M\times n_M} & \boldsymbol{O} \\ \boldsymbol{O} & \boldsymbol{m}_{n_m\times n_m} \end{bmatrix}\boldsymbol{l}\boldsymbol{a} \qquad (1)$$

where $\boldsymbol{X}$ and x are displacement vector of the main structure and TMDs; $\boldsymbol{l}$ is the location matrix with all 0 elements except the unit elements at jth row and pth column, where j takes 1, 2, ⋯, n_m and p is the label representing the order of the main structure DOFs that interacts with the sub-oscillators.$\boldsymbol{\iota}=[\boldsymbol{I}_{3\times3}, \boldsymbol{I}_{3\times3}, \cdots, \boldsymbol{I}_{3\times3}]^{\mathrm{T}}$ and $\boldsymbol{I}_{3\times3}$ is a 3×3 unit matrix; $\boldsymbol{a}=[a_{\mathrm{X}},a_{\mathrm{Y}},a_{\mathrm{Z}}]^{\mathrm{T}}$ is accelerations; T is transpose.

By transforming only the main structure to its modal space, i.e., using the transformation in Eq. (2), and performing mode truncation[12], one has the dynamic equation for the simplified NC-MTMD system (Fig. 1) as Eq. (3).

$$\begin{bmatrix} \boldsymbol{X} \\ \boldsymbol{x} \end{bmatrix} = \hat{\boldsymbol{\Phi}} \begin{bmatrix} \boldsymbol{q} \\ \boldsymbol{x} \end{bmatrix} = \begin{bmatrix} \boldsymbol{\Phi}_{n_M \times n_{\overline{M}}} & \boldsymbol{O} \\ \boldsymbol{O} & \boldsymbol{I}_{n_m \times n_m} \end{bmatrix} \begin{bmatrix} \boldsymbol{q} \\ \boldsymbol{x} \end{bmatrix} \tag{2}$$

where $\boldsymbol{\Phi}_{n_M \times n_{\overline{M}}}$ is the mode matrix that composed of $n_{\overline{M}}$ modes of the main structure; $\boldsymbol{I}_{n_m \times n_m}$ is unit matrix; $\boldsymbol{q}$ is generalized coordinate of the main structure.

$$\begin{bmatrix} \overline{M}_{n_{\bar{M}} \times n_{\bar{M}}} & \boldsymbol{O} \\ \boldsymbol{O} & m \end{bmatrix} \begin{bmatrix} \ddot{q} \\ \ddot{x} \end{bmatrix} + \begin{bmatrix} \overline{C}_{n_{\bar{M}} \times n_{\bar{M}}} + \boldsymbol{\Phi}^{\mathrm{T}} l^{\mathrm{T}} \boldsymbol{cl\Phi} & -\boldsymbol{\Phi}^{\mathrm{T}} l^{\mathrm{T}} c \\ -\boldsymbol{cl\Phi} & c \end{bmatrix} \begin{bmatrix} \dot{q} \\ \dot{x} \end{bmatrix} + \begin{bmatrix} \overline{K}_{n_{\bar{M}} \times n_{\bar{M}}} + \boldsymbol{\Phi}^{\mathrm{T}} l^{\mathrm{T}} \boldsymbol{kl\Phi} & -\boldsymbol{\Phi}^{\mathrm{T}} l^{\mathrm{T}} \boldsymbol{k} \\ -\boldsymbol{kl\Phi} & \boldsymbol{k} \end{bmatrix} \begin{bmatrix} q \\ x \end{bmatrix} = \hat{\boldsymbol{\Phi}}^{\mathrm{T}} \begin{bmatrix} \boldsymbol{M} & \boldsymbol{O} \\ \boldsymbol{O} & m \end{bmatrix} \boldsymbol{\iota a} \tag{3}$$

where $\overline{M} = \boldsymbol{\Phi}^{\mathrm{T}} \boldsymbol{M} \boldsymbol{\Phi} = \mathrm{diag}\{\overline{M}_1, \overline{M}_2, \cdots, \overline{M}_{n_{\overline{M}}}\}$, $\overline{\boldsymbol{C}} = \boldsymbol{\Phi}^{\mathrm{T}} \boldsymbol{C} \boldsymbol{\Phi}$ and $\overline{K} = \boldsymbol{\Phi}^{\mathrm{T}} \boldsymbol{K} \boldsymbol{\Phi} = \mathrm{diag}\{\overline{K}_1, \overline{K}_2, \cdots, \overline{K}_{n_{\bar{M}}}\}$.$\overline{C} = \mathrm{diag}\{\overline{C}_1, \overline{C}_2, \cdots, \overline{C}_{n_{\overline{M}}}\}$ if the main structure has proportional damping.

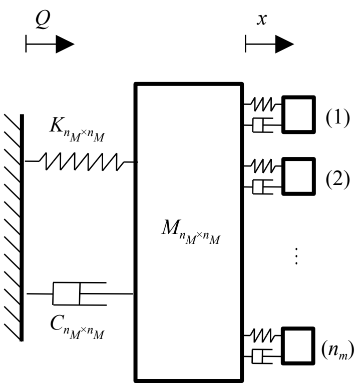

Fig. 1 NC-MTMD system

The uncertainty ubiquitously exists in the structural system and therefore the structural random variable set can be expressed as Eq. (4).

$$\boldsymbol{\psi}_S = \{\boldsymbol{M}, \boldsymbol{C}, \boldsymbol{K}, \boldsymbol{m}, \boldsymbol{c}, \boldsymbol{k}\} \tag{4}$$

2 Earthquake hazard model

Stationary Kanai-Tajimi (KT) model[13] was adopted to model the ground motion excitation. A three-dimensional filter, with one DOF in each direction, was assembled to the NC-MTMD system. For simplification, the filter was assumed to be isotropic and expressed as Eq. (5),

$$\begin{cases} \boldsymbol{I}_{3\times3}\ddot{x}_{\mathrm{f}} + 2\xi_{\mathrm{f}}\omega_{\mathrm{f}}\boldsymbol{I}_{3\times3}\dot{x}_{\mathrm{f}} + \omega_{\mathrm{f}}^2\boldsymbol{I}_{3\times3}x_{\mathrm{f}} = -\boldsymbol{w} \\ a = \ddot{x}_{\mathrm{f}} + w = -\left(2\xi_{\mathrm{f}}\omega_{\mathrm{f}}\dot{x}_{\mathrm{f}} + \omega_{\mathrm{f}}^2 x_{\mathrm{f}}\right) \end{cases} \tag{5}$$

where x_{f} is the displacement vector of the KT filter; ξ_{f} and ω_{f} are the damping ratio and circular frequency of the KT filter, respectively; $\boldsymbol{w} = \begin{bmatrix} w_X & w_Y & w_Z \end{bmatrix}^{\mathrm{T}}$ is the bed rock white noise excitation.

Substitute Eq. (5) into Eq. (3), one has Eq. (6),

$$\boldsymbol{M}_{\mathrm{ft}} \begin{bmatrix} \ddot{q} \\ \ddot{x} \\ \ddot{x}_{\mathrm{f}} \end{bmatrix} + \boldsymbol{C}_{\mathrm{ft}} \begin{bmatrix} \dot{q} \\ \dot{x} \\ \dot{x}_{\mathrm{f}} \end{bmatrix} + \boldsymbol{K}_{\mathrm{ft}} \begin{bmatrix} q \\ x \\ x_{\mathrm{f}} \end{bmatrix} = \boldsymbol{f}_{\mathrm{bw}} \tag{6}$$

where $\boldsymbol{M}_{\mathrm{ft}}$, $\boldsymbol{C}_{\mathrm{ft}}$, $\boldsymbol{K}_{\mathrm{ft}}$ and $\boldsymbol{f}_{\mathrm{bw}}$ are the mass, damping, stiffness matrix and load vector for the NC-MTMD system with the incorporation of the KT filter, respectively, and they are given by:

$$\boldsymbol{M}_{\mathrm{ft}} = \begin{bmatrix} \overline{M} & \boldsymbol{O} & \boldsymbol{O} \\ \boldsymbol{O} & \boldsymbol{m} & \boldsymbol{O} \\ \boldsymbol{O} & \boldsymbol{O} & \boldsymbol{I}_{3\times3} \end{bmatrix} \tag{7}$$

$$\boldsymbol{C}_{\mathrm{ft}} = \begin{bmatrix} \overline{\boldsymbol{C}} + \boldsymbol{\Phi}^{\mathrm{T}} l^{\mathrm{T}} cl\boldsymbol{\Phi} & -\Phi^{\mathrm{T}} l^{\mathrm{T}} c & -2\boldsymbol{\Phi}^{\mathrm{T}}\boldsymbol{M}\boldsymbol{\iota}_{n\times3}\xi_{\mathrm{f}}\omega_{\mathrm{f}} \\ -cl\boldsymbol{\Phi} & c & -2\boldsymbol{m}\boldsymbol{\iota}_{n_m\times3}\xi_{\mathrm{f}}\omega_{\mathrm{f}} \\ \boldsymbol{O} & \boldsymbol{O} & 2\xi_{\mathrm{f}}\omega_{\mathrm{f}}\boldsymbol{I}_{3\times3} \end{bmatrix} \tag{8}$$

$$\boldsymbol{K}_{\mathrm{ft}} = \begin{bmatrix} \overline{K} + \boldsymbol{\Phi}^{\mathrm{T}} l^{\mathrm{T}} \boldsymbol{kl\Phi} & -\boldsymbol{\Phi}^{\mathrm{T}} l^{\mathrm{T}} k & -\boldsymbol{\Phi}^{\mathrm{T}}\boldsymbol{M}\boldsymbol{\iota}_{n\times3}\omega_{\mathrm{f}}^2 \\ -\boldsymbol{kl\Phi} & \boldsymbol{k} & -\boldsymbol{m}\boldsymbol{\iota}_{n_m\times3}\omega_{\mathrm{f}}^2 \\ \boldsymbol{O} & \boldsymbol{O} & \omega_{\mathrm{f}}^2\boldsymbol{I}_{3\times3} \end{bmatrix} \tag{9}$$

$$\boldsymbol{f}_{bw} = \begin{bmatrix} \boldsymbol{O}_{1\times(n+n_l)} & -\boldsymbol{w}^{\mathrm{T}} \end{bmatrix}^{\mathrm{T}} \tag{10}$$

Three components of earthquake excitation are not necessarily correlated in its principle directions. With S_0 denoting the main direction intensity of earthquake excitation, Penzien and Watabe[14] assigned the ratio of variance in three directions as 1: 0.75: 0.5, and therefore the excitation power spectrum density matrix $\boldsymbol{S}$ can be defined as Eq. (11).

$$\boldsymbol{S} = E\left(\boldsymbol{w}\boldsymbol{w}^{\mathrm{T}}\right) = \begin{bmatrix} S_0 & 0 & 0 \\ 0 & 0.75S_0 & 0 \\ 0 & 0 & 0.5S_0 \end{bmatrix} \tag{11}$$

where $E(\bullet)$ is expectation operator.

Amplitude and duration are important characters of ground motion.In this paper, the amplitude was expressed as a function of peak ground acceleration (PGA).Assuming that PGA takes 3 times of acceleration variance σ_w[15], one has the expression of S_0 as Eq. (12).

$$S_0 = \frac{2\xi_{\mathrm{f}}(PGA)^2}{3^2\pi\left(1+4\xi_{\mathrm{f}}^2\right)\omega_{\mathrm{f}}} \tag{12}$$

PGA is a function of earthquake magnitude M_s and focal distance R[16–18] and was assumed to be expressed as Eq. (13).

$$PGA = b_1 e^{b_2 M_s} (R + R_0)^{-b_3} \tag{13}$$

where b_1, b_2, b_3 and R_0 are parameters obtained from estimation over rather broad geographical regions.

The probability model of moment magnitude M_s can be described using truncated Gutenberg-Richter relationship[19] in the interval of $[M_{s\min}, M_{s\max}]$, as Eq. (14).

$$p(M_s) = \frac{\beta_{M_s} e^{-\beta_{M_s} M_s}}{e^{-\beta_{M_s} M_{s\min}} - e^{-\beta_{M_s} M_{s\max}}} \tag{14}$$

where β_{M_s} is the regional seismicity factor and $p(M_s)$ is the annual frequency.

The ground-motion duration t_d was assumed to be composed of the source duration and path-dependent duration T_p[20], as Eq. (15).

$$t_d = T_p + 0.5/f_a \tag{15}$$

where f_a is corner frequency.

Considering the uncertainty that associated in ω_f, ξ_f, R, Ms, the hazard random variable set can be expressed as Eq. (16).

$$\psi_H = \{\omega_f, \xi_f, M_s, R\} \tag{16}$$

Strictly speaking, the random variables should also include the bed rock white noise process. However, the structural response under random process can be solved by stochastic dynamics and eventually be expressed as a deterministic response variance. Therefore, it was not included in the random variable set.

3 Reliability Analyses

The state vector for the NC-MTMD system with the KT filter is $\boldsymbol{y} = [\ q \quad x \quad x_f \quad \dot{q} \quad \dot{x} \quad \dot{x}_f\ ]^T$ and one can easily obtain the state function of the structure, as Eq. (17).

$$\dot{\boldsymbol{y}} = \boldsymbol{A}\boldsymbol{y} + \boldsymbol{B}\boldsymbol{f}_{bw} \tag{17}$$

where $\boldsymbol{A}$ and $\boldsymbol{B}$ are state matrices given by

$$\boldsymbol{A} = \begin{bmatrix} \boldsymbol{O} & \boldsymbol{I} \\ -\boldsymbol{M}_{ft}^{-1}\boldsymbol{K}_{ft} & -\boldsymbol{M}_{ft}^{-1}\boldsymbol{C}_{ft} \end{bmatrix}, \boldsymbol{B} = \begin{bmatrix} \boldsymbol{O} \\ \boldsymbol{M}_{ft}^{-1} \end{bmatrix} \tag{18}$$

The stationary response can be obtained by solving the Lyapunov equation, as Eq. (19).

$$\boldsymbol{A}\boldsymbol{R} + \boldsymbol{R}\boldsymbol{A}^T + 2\pi \begin{bmatrix} \boldsymbol{O} & \boldsymbol{O} \\ \boldsymbol{O} & \boldsymbol{S} \end{bmatrix} = \boldsymbol{O} \tag{19}$$

where $\boldsymbol{R}$ is the covariance matrix of $\boldsymbol{y}$.

The response corresponding to certain state variable $z_i (i = 1, 2, , n_z)$ can be calculated as Eq. (20).

$$\begin{cases} \sigma_{z_i}^2 = \boldsymbol{n}_i^T \boldsymbol{G}\boldsymbol{R}\boldsymbol{G}^T \boldsymbol{n}_i, \\ \sigma_{\dot{z}_i}^2 = \boldsymbol{n}_i^T \boldsymbol{G}\boldsymbol{A}\boldsymbol{R}\boldsymbol{A}^T \boldsymbol{G}^T \boldsymbol{n}_i \end{cases} \tag{20}$$

where $\sigma_{z_i}^2$ and $\sigma_{\dot{z}_i}^2$ are variance of variable z_i and its first derivative of time, respectively; $\boldsymbol{G}$ is observation matrix; $\boldsymbol{n}_i$ is unit vector at the dimension of variable z_i, therefore $z_i = \boldsymbol{n}_i^T \boldsymbol{z}$.

Take structure performance space Π as a n_z dimensions space with every dimension corresponding to a state variable and assume that every variable has a certain limit state bound β_i, one therefore has a hypercube space Π_s named safe polygon, in which all structure variables satisfies the limit state condition, as Eq. (21).

$$\Pi_s = \{z \in R : |z_i| < \beta_i\}, i = 1, 2, \cdots, n_z \tag{21}$$

The first passage failure probability was expressed as Eq. (22).

$$P_f(t_d) = \int_0^T P[z(\tau) \notin \Pi_s] d\tau = 1 - \exp(-v_z^+ t_d) \tag{22}$$

where v_z^+ is the out-crossing rate and can be calculated from Eq. (23).

$$\begin{cases} v_z^+ \approx \sum_{i=1}^{n_z} w_{z_i} \left(\lambda_{z_i} r_{z_i}^+ \right), \\ w_{z_i} = \int_{B_i \cap F} p(z_\perp | z_i = \beta_i) dz_\perp, \\ r_{z_i}^+ = \dfrac{\sigma_{\dot{z}_i}}{\pi \sigma_{z_i}} \exp\left\{ -\dfrac{\beta_i^2}{2\sigma_{z_i}^2} \right\}, \\ \lambda_{z_i} \approx \dfrac{1 - \exp\left\{ -q^{0.6} \left(\dfrac{2}{\sqrt{\pi}} \right)^{0.1} \dfrac{2\sqrt{2}}{n_b} \dfrac{\beta_i}{\sigma_{z_i}} \right\}}{1 - \exp\left(-\beta_i^2 / 2\sigma_{z_i}^2 \right)}, \\ q = \dfrac{\sigma_{z_i}^5}{4\pi \int_{-\infty}^{+\infty} |\omega| S_{z_i z_i}(\omega) d\omega \int_{-\infty}^{+\infty} S_{z_i z_i}^2(\omega) d\omega} \end{cases} \tag{23}$$

where w_{z_i} is the correlation weighting factor and can be obtained by Eq. (23)[21], $\boldsymbol{z}_\perp = \boldsymbol{z} - z_i \boldsymbol{n}_i$, B_i is the limit state hyperplane bound of z_i and F is the surface of hypercube space Π_s; Eq. (23) is the Rice function[22–23] and yields unconditional out-crossing rate; λ_{z_i} is the out-crossing correction factor that calculated by Eq. (23)[24], n_b is the number of limit state bound side; factor q can be calculated by Eq.(23)[21], ω is circular frequency and $S_{z_i z_i}(\omega)$ is the power spectrum density of structural response z_i.

Noting that the duration of earthquake is a function of hazard variables[20], the unconditional failure probability can be obtained by the integration as Eq. (24).

$$P_{\mathrm{f}}=\int\int p_{\mathrm{f}}(t_{\mathrm{d}}(\psi_{\mathrm{H}})/\{\psi_{\mathrm{S}},\psi_{\mathrm{H}}\})\,p(\psi_{\mathrm{S}})\,p(\psi_{\mathrm{S}})\,\mathrm{d}\psi_{\mathrm{H}}\mathrm{d}\psi_{\mathrm{H}} \tag{24}$$

Assuming failure event follows engineering Poisson distribution of independent occurrences[25], the failure probability after a time period t_{l} can be obtained by Eq. (25).

$$\begin{cases} P_{\mathrm{F}}(t_{\mathrm{l}})=1-\mathrm{e}^{-t_{\mathrm{l}}\nu_{\mathrm{f}}P_{\mathrm{f}}}, \\ \nu_{\mathrm{f}}=\mathrm{e}^{\alpha_{M_{\mathrm{s}}}-\beta_{M_{\mathrm{s}}}M_{\mathrm{s}\min}}-\mathrm{e}^{\alpha_{M_{\mathrm{s}}}-\beta_{M_{\mathrm{s}}}M_{\mathrm{s}\max}} \end{cases} \tag{25}$$

where $\alpha_{M_{\mathrm{s}}}$ and $\beta_{M_{\mathrm{s}}}$ are regional seismicity factors.

4 Optimization

With given limit state bounds, the objective function that adopted in this paper was defined as P_{F}.With design variables as $\boldsymbol{\theta}$, the optimization problem can be described as a constrained optimization problem as Eq. (26).

$$\begin{cases} \min P_F(\boldsymbol{\theta}), \\ \theta=\{\ \omega_1,\omega_2,\cdots,\omega_{n_m}\quad \xi_1,\xi_2,\cdots,\xi_{n_m}\ \}, \\ \theta\in \bigcap_{j=1}^{n_m}\{\{\omega_j:\omega_j\in[\omega_{j\min},\omega_{j\max}]\}\cap\{\xi_j:\xi_j\in[\xi_{j\min},\xi_{j\max}]\}\} \end{cases} \tag{26}$$

where $\omega_j=\sqrt{k_j/m_j}$ and $\xi_j=c_j/(2m_j\omega_j)$.

5 Case study

The case considered here is a concentrically braced steel thermal power plant building (Fig. 2). The structure consists of boiler frames, air heater houses and a scuttle bay. In its scuttle bay, 7 scuttles with each weight 1 098.3 tons locate at 32.2 m height of the structure.

5.1 Deterministic model

The structure was located at a Chinese site with relatively high hazard level. The expected bounds of earthquake magnitude are M_{smin}=5.5 and M_{smax}=8, respectively. The regional seismicity factors $\alpha_{M_{\mathrm{s}}}$ and $\beta_{M_{\mathrm{s}}}$ are 4ln(10) and 2.16[16], respectively.In Eq.(13), b_1=6.63; b_2=1.17; b_3=-1.43; R_0=14 for PGA in cm/s^2[18]. In Eq. (15) $f_{\mathrm{a}}=10^{2.181-0.496M_{\mathrm{s}}}$[26] and $T_{\mathrm{p}}=0.05R$[27]. The site was 40 km away from the focal center. The soil condition fits class III (stiff soil) with predominant period of 0.55 s. The KT filter parameters were assigned as $\xi_{\mathrm{f}}=0.6$[28] and $\omega_{\mathrm{f}}=3.63\pi$ rad/s (the corresponding circular frequency of the predominant period).

The main structure was modeled by its first 12 modes, at which the cumulated participation factor at two horizontal directions is larger than 90% (Tab. 1). Rayleigh damping was adopted to model the inherent damping of the main structure, with 2% at 0.1 s and 1 s[29], respectively. Scuttles were modeled as a 2DOF lumped mass each, with a DOF at each horizontal direction.

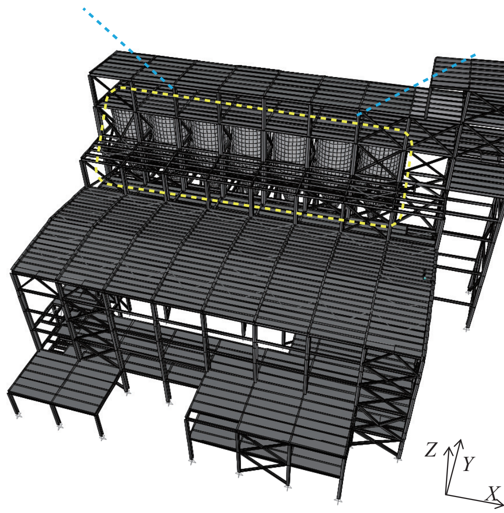

(a) entire structure

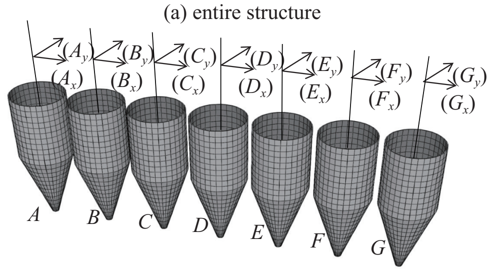

(b) scuttles

Fig. 2 Thermal power plant

Tab. 1 Dynamic properties of the main structure

r	$\overline{T}_r$	$\overline{\omega}_r$	$\sum\Gamma_X$/%	$\sum\Gamma_Y$/%
1	1.35	4.65	41	4
2	1.26	4.99	50	42
3	1.02	6.16	52	69
4	0.80	7.85	57	74
5	0.66	9.52	57	82
6	0.62	10.13	72	86
7	0.55	11.42	75	86
8	0.54	11.64	77	90
9	0.48	13.09	79	90
10	0.41	15.32	79	90
11	0.41	15.32	88	90
12	0.38	16.53	91	91

Note: $\overline{T}_r$ (s) and $\overline{\omega}_r$ (rad/s) are natural periods and circular frequencies of the main structure,with $\overline{\omega}_r=2\pi/\overline{T}_r=\sqrt{\overline{M}_r/\overline{K}_r}$;$\sum\Gamma_X$ and $\sum\Gamma_Y$ are cumulate mode participation factors of the main structure in X and Y direction,respectively.

5.2 Probabilistic model

Parameters in random variable sets Ψ_{S} and Ψ_{H} were modeled as random variables with probabilistic distributions in Tab. 2. Random elements in each matrices ($\overline{M}$ and $\overline{K}$) were assumed to be perfectly correlated to reduce the prohibitive computational burden. Scuttle mass is modeled by Beta distribution for its bounded character.Mass, stiffness and damping of scuttles were assumed to be independent with each other. Besides specific probabilistic distributions, all the rests were using the Lognormal distribution for its wide application and non-negative domain (Fig. 3).

Tab. 2　Probabilistic models of input parameters

Class	Variable	Probabilistic model	*CoV*/%
Hazard	M_s	Eq. (14)	—
	R	Lognormal	40
	ω_f	Lognormal	30
	ξ_f	Lognormal	30
Main structure	$\overline{M}$	Lognormal	10
	$\overline{K}$	Lognormal	10
	$\overline{C}$	Lognormal	30
Scuttles	m	Beta	32
	k	Lognormal	10
	c	Lognormal	15

Note: 1) *CoV* is coefficient of variance; 2) All the variables take their mean values as that of the deterministic model.

Latin hypercube sampling (LHS) strategy was adopted in this paper to reduce the needed sample size. Appropriate sample size investigation was further carried out to determine the necessary sample size.With design variables $\omega_j=\{0.3\omega_{j\max}+0.7\omega_{j\min}, 0.7\omega_{j\max}+0.3\omega_{j\min}\}$ and $\xi_j=\{0.3\xi_{j\max}+0.7\xi_{j\min}, 0.7\xi_{j\max}+0.3\xi_{j\min}\}$, 128 combinations/cases were generated, with the consideration of computational burden and representativeness. Normalized probability, which is defined as the ratio between the probabilities P_F^e estimated by using certain number and P_F^∞ by all of the samples, was used to assess the estimation accuracy of using the certain number of samples. The appropriate sample size is required to have P_F^e/P_F^∞ of all cases in [90%, 110%]. From Fig. 4, it can be found that 4 699 samples are enough. Therefore, 4 699 samples were generated in the following studies.

5.3　Statement of optimization problem

Considering that a too high dimensional structural output may cause a prohibitive computational burden, only eight structural outputs that expected to be the most critical, i.e., drifts of corner columns at the 1st and 3th floor (shown in Fig. 5), were considered, which are expected to have higher value[30].

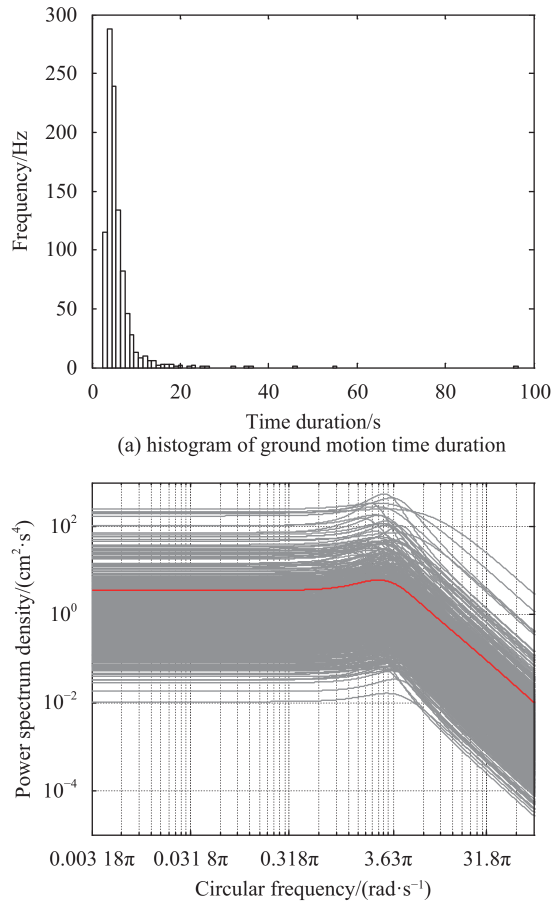

(a) histogram of ground motion time duration

(b) power spectrum density samples

Fig. 3　Sampled ground motion characters

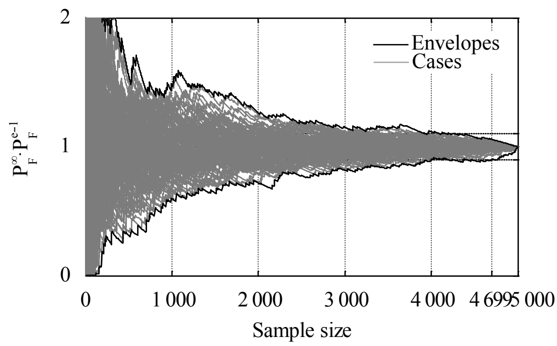

Fig. 4　Appropriate sample size study

Denoting $j=1,2,\cdots,n_m$ in Eq.(26) as $\{A_x, A_y, \ldots, G_y\}$ (Fig.2(b)), the optimization problem can be expressed as Eq.(27).

$$\begin{cases}\min P_F(\boldsymbol{\theta}) \\ \theta=\{\ \omega_{A_x},\omega_{A_y},\cdots,\omega_{G_y}\quad \xi_{A_x},\xi_{A_y},\cdots,\xi_{G_y}\ \}, \\ \theta\in \underset{j=\{A_x,A_y,\cdots,G_y\}}{I}\{\{\omega_j:\omega_j\in[\omega_{j\min},\omega_{j\max}]\}\cap\{\xi_j:\xi_j\in[\xi_{j\min},\xi_{j\max}]\}\}\end{cases} \tag{27}$$

where $\omega_{j\min}$, $\omega_{j\max}$, $\xi_{j\min}$, $\xi_{j\max}$ takes 0, 17 rad/s, 0, 0.3, respectively[6].

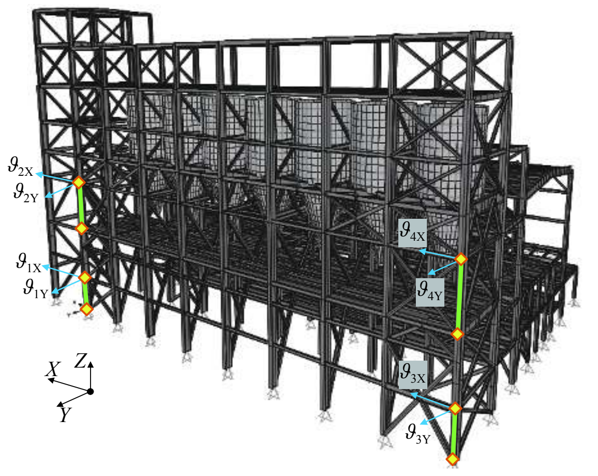

Fig. 5 Structural drifts

5.4 Optimum design

The problem contains uncertainty and deterministic algorithms (e.g., the gradient-based algorithms and direct search algorithms) are not fit for this situation. The genetic algorithm, which is one of the most popular stochastic optimization algorithms, was adopted in this paper to solve the optimization problem.

The optimum design obtained by the optimization process was summarized in Tab. 3.

Tab. 3 Optimum Design

DOF	ω_{opt}	ξ_{opt}/%	DOF	ω_{opt}	ξ_{opt}/%
A_x	13.96	22.40	A_y	2.62	11.05
B_x	11.33	13.23	B_y	8.24	1.68
C_x	3.08	28.71	C_y	13.82	0.15
D_x	2.29	8.76	D_y	5.48	13.40
E_x	15.86	1.02	E_y	0.81	5.09
F_x	16.09	22.35	F_y	12.48	11.52
G_x	6.79	12.99	G_y	6.86	16.56
P_F			5.435 1%		

It can be seen that ω_{opt} varies over the range of natural periods of the main structure, which highlights the importance of higher modes. There is no obvious trend with ξ_{opt}. But comparing with the results in[6], which assumed no uncertainty, most ξ_{opt} here in Tab. 3 are higher. This is because that higher damping ratio enhances robustness of MTMD[31] and therefore benefits its performance when uncertainty presents.

6 Parametric studies

Uncertain mass of the scuttles caused by changing coal storage cause large variation on oscillator frequencies.The variation can further cause problem on tuning. Pendulum system has an independent period with system mass, because of the perfect correlation between stiffness and mass. Consequently, the pendulum strategy is potentially a solution for the mass uncertainty. Another important practical problem is collision between coal scuttles and its surrounding structural members. These two important practical aspects were therefore investigated in this section.

6.1 Influence of oscillator type

For translational MU-NC-MTMD system (Fig. 6), stiffness of sub-oscillators was induced by elastic potential energy of isolators. As an alternative, the pendulum MU-NC-MTMD, in which stiffness of sub-oscillators is the function of gravity potential energy of oscillators, can possibly be effective to enhance the system robustness when mass uncertainty presents.

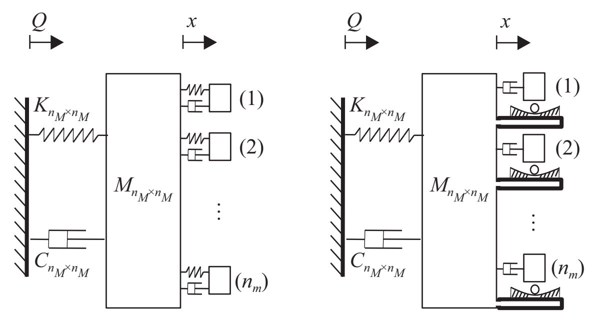

(a) Translational MU-NC-MTMD (b) Pendulum MU-NC-MTMD

Fig. 6 Translational MU-NC-MTMD and pendulum MU-NC-MTMD

For pendulum MU-NC-MTMD, all modeling methods are same as translational MU-NC-MTMD, but stiffness. For pendulum MU-NC-MTMD, stiffness was expressed as Eq. (28).

$$k = \mathrm{diag}\{m_1 g/\rho_1, m_2 g/\rho_2, \cdots, m_{n_m} g/\rho_{n_m}\} \tag{28}$$

where g and ρ denote gravity acceleration and length of pendulums, respectively.

$1/\rho$ of each scuttle was assumed to follow lognormal distribution, with the CoV of 0%, 5% and 10% for three different cases, respectively.

It can be observed from Tab. 4 that the translational system has slightly smaller P_F than the pendulum system. Furthermore, P_F of pendulum system is not sensitive to the uncertainty of $1/\rho$.

6.2 Influence of seismic gap

The gap between the coal scuttle and the surrounding structural members is 130 mm. Considering possible collision in $\{A_x, A_y, \cdots, G_y\}$ directions, 14 additional relative displacement limit state bounds were included.

Tab. 4　Failure probabilities of translational and pendulum MU-NC-MTMD system

Cases	$CoV(1/\rho)$/%	P_F/%
Translational system		5.435 1
Pendulum system	0	5.768 7
	5	5.711 6
	10	5.802 3

For the optimum design in Tab. 3, probability of failure with the consideration of collision P_{Fc} was calculated, which equals 8.11%. The consideration of collision slightly increased the failure probability, which suggests that collision problem is not that critical. It is also possible to optimize P_{Fc} to obtain a design that mitigates both P_F and collision problem.

The author adopted multi-objective method[5] in a previous engineering problem. The multiple output unconditional PF integrates multiple objectives into one failure probability and therefore avoids cumbersome multi-objective optimization.

7　Conclusion

In this paper, a multiple output unconditional reliability-based design framework for nonconventional multiple tuned mass damper for a complex structure was proposed. With the description of simplified structure model and earthquake hazard model, a multiple output reliability method was presented. Optimization problem was then formulated. A case of coal scuttles isolation for thermal power plant was solved to illustrate the method. From the study, conclusions as follows can be drawn:

1) The framework adopts failure probability with multiple limit state bounds as the objective function and therefore avoids the cumbersome multi-objective optimization. Multiple responses are integrated into one failure probability, which is clearer.

2) The pendulum system does not perform better than translational system in the case with equal uncertainty. Performance of pendulum system is not sensitive to the degree of its curvature uncertainty.

3) Collision problem is not critical for this case but it does affect the failure probability. Failure probability with the consideration of collision can be further optimized to search a design solution that mitigates both structural failure probability and collision problem.

References:

[1] O'Rourke T D.Lessons learned for lifeline engineering from major urban earthquakes[C]//11th World Conference on Earthquake Engineering,Acapalco,1996.

[2] Muto K,Shibata K,Tsugawa T,et al.Earthquake resistant design of boiler building of thermal power plant[C]//Proceedings of Ninth World Conference on Earthquake Engineering,Tokyo-Kyoto,1988,6:855–860.

[3] Wang J.Seismic performance-based design and risk analysis of thermal power plant building with consideration of vertical and mass irregularities[J].Engineering Structures,2018, 164:141–154.

[4] Rajeev P.Effects of vertical irregularities and construction quality in seismic fragilities for reinforced concrete buildings[J].International Journal of Earthquake and Impact Engineering,2017,2:1–31.

[5] Dai K.Optimal probability-based partial mass isolation of elevated coal scuttle in thermal power plant building[J].The Structural Design of Tall and Special Buildings,2018:e1477.

[6] Li B,Dai K,Li H,et al.Optimum design of a non-conventional multiple tuned mass damper for a complex power plant structure [J].Engineering Structures,2018,Submitted.

[7] Shu Z.Optimum seismic design of a power plant building with pendulum tuned mass damper system by its heavy suspended buckets[J].Engineering Structures,2017,136: 114–132.

[8] Jensen H.TMDs for vibration control of systems with uncertain properties[J].Journal of Structural Engineering,1992, 118:3285–3296.

[9] Matta E.Seismic performance of pendulum and translational roof-garden TMDs[J].Mechanical Systems and Signal Processing,2009,23:908–921.

[10] Rathi A.Reliability-based performance optimization of TMD for vibration control of structures with uncertainty in parameters and excitation[J].Structural Control and Health Monitoring,2017,24(1):e1857.

[11] Igusa T.Response of uncertain systems to stochastic excitations[J].ASCE Journal of Engineering Mechanics,1988, 114:812–832.

[12] Lin J.Precise and efficient computation of complex structures with TMD devices[J].Journal of Sound and Vibration,1999,223:693–701.

[13] Tajimi H.A statistical method of determining the maximum response of a building during earthquake [C]//Proceedings of 2nd World Conference on Earthquake Engineering,Tokyo,1960.

[14] Penzien J.Characteristics of 3-Dimensional earthquake

ground motions[J].Earthquake Engineering and Structural Dynamics,1974,3:365–373.
[15] Marano G.Multiobjective optimization criteria for linear structures subject to random vibrations[J].The Open Civil Engineering Journal,2008,2:75–87.
[16] Esteva L.Spectra of earthquakes at moderate and large distances[J].Society of Mexico de Ing.Seismica,1954,2:1–18.
[17] Kanai K.An empirical formula for the spectrum of strong Earthquake motions[J].Balletin of the Earthqaake Reseach Institute, Unicersity of Tokyo,1961,39:85–95.
[18] Huo J.Study on attenuation laws of ground motion parameters[J].Earthquake Engineering and Engineering Vibration,1992,12:1–11.
[19] Cornell C.A.,Vanmarcke E.H.The major influences on seismic risk [C]//Proceedings of the fourth world conference on earthquake engineering,1969,1:69–83.
[20] Boore D.Simulation of ground motion using the stochastic method[J].Pure and applied geophysics,2003,160:635–676.
[21] Taflanidis A A,Beck J L.Analytical approximation for stationary reliability calculation of linear dynamic systems (EERL Report No.2005-3) [R].California:California Institute of Technology,2005.
[22] Rice S.Mathematical analysis of random noise[J].Bell Labs Technical Journal,1944,23:282–332.
[23] Rice S.Mathematical analysis of random noise[J].The Bell System Technical Journal,1945,24:46–156.
[24] Vanmarcke E.On the distribution of the first passage time for normal stationary processes[J].Journal of Applied Mechanics,1975,42:215–220.
[25] Papadimitriou C.Effects of structural uncertainties on TMD design:a reliability-based approach[J].Journal of Structure Control,1997,4:65–88.
[26] Atkinson G.Stochastic modeling of california ground motions[J].Balletin of the Seismological Soeiety of America, 2000,90(90):255–274.
[27] Taflanidis A.A simulation-based framework for risk assessment and probabilistic sensitivity analysis of base-isolated structures[J].Earthquake Engineering and Structural Dynamics,2011,40:1629–1651.
[28] Yu Z.,Cao G.Random vibration theory and its application [M].Shanghai,Tongji University Press,1988.
[29] Kumar A,Ashwin Kumar P C,Sahoo D R.Response of staggered arrangement of concentric braces using perform-3D [C]//8th International Conference on Behavior of Steel Structures in Seismic Areas,Shanghai,2015.
[30] Dai K.Elasto-plastic analysis of a large braced frame steel power plant structure[J].China Civil Engineering Journal, 2016(S2):1–6.
[31] Hoang N.Design of multiple tuned mass dampers by using a numerical optimizer[J].Earthquake Engineering and Structural Dynamics,2005,34:125–144.

戴靠山，男，2009年博士毕业于美国北卡罗来纳大学，2009—2011年,在美国北卡大学及加州灾害风险管理高科技公司进行短期研究工作，2011—2017年,在同济大学任教，为土木工程学院副教授、博士生导师、院长助理，土木工程防灾国家重点实验室成员；2018年起调入四川大学任建筑与环境学院土木系主任、教授。曾获2013年度国际试验力学协会Harting Award，是加拿大西安大路大学土木与环境工程系客座研究教授。其研究兴趣包括能源基础设施防灾、新型检测监测技术在土木工程中的应用、基于波传的场地评估等。主持多项科研项目，针对大型电力设施韧性，工程结构抗震抗风，隔震减震和振动控制开展研究工作。他同时在房屋检测评价改造、基于地震法的勘察、及工程监测新技术等交叉学科方面进行积极探索。

（编辑　黄小川）

引用格式：Dai Kaoshan,Li Bowei,Li Huiying,et al.Reliability based mss uncertain nnconventional multiple tuned mass damper optimization for thermal power plant[J].Advanced Engineering Sciences,2018,50(3):82–90.[戴靠山,李伯维,李卉颖,等.用于火电厂减震的变质量MTMD基于可靠度的优化[J].工程科学与技术,2018,50(3):82–90.]